Ali Shokuhi Rad*, Mehri Esfahanian, Etesam Ganjian, and Habib-allah Tayebi

Ab-Initio Study of Physisorption of Hydrogen Cyanide on 2PANI: a Model for Polyaniline Gas Sensor

DOI 10.1515/zpch-2015-0645
Received June 11, 2015; accepted April 7, 2016

Abstract: We investigated the adsorption properties of HCN on dianiline (as a model for polyaniline, denoted here as 2PANI) using density functional theory (DFT) by considering the geometry as well as the electronic property. Contact information of 2PANI with HCN at different configurations was studied and the adsorption energy was calculated in each case. UV-vis analysis, density of states (DOS) and natural bond orbital (NBO) analysis were used to study the interaction of HCN with 2PANI at different configurations. Our calculations showed that HCN could be adsorbed on 2PANI with adsorption energy of ~ -4.3 kcal mol^{-1} (based on counterpoise corrected energy). Based on our results we suggest polyaniline as a potential polymeric sensor for HCN detection.

Keywords: DFT, Physisorption, Hydrogen Cyanide, Polyaniline.

1 Introduction

Conducting polymers including polyacetylene [1], polypyrole [2], polythiophene, poly (3,4-ethylenedioxythiophene) [3], and polyaniline [4] are comprehensively considered as gas sensors owing to their mechanical strength and remarkable

***Corresponding author: Ali Shokuhi Rad,** Department of Chemical Engineering, Qaemshahr Branch, Islamic Azad University, Qaemshahr, Iran, e-mail: a.shokuhi@gmail.com
Mehri Esfahanian: Department of Chemical Engineering, Qaemshahr Branch, Islamic Azad University, Qaemshahr, Iran
Etesam Ganjian: Department of Chemical Engineering, Babol Noshirvani University of Technology, Babol, Iran
Habib-allah Tayebi: Faculty of Textile and Apparel Engineering, Qaemshahr Branch, Islamic Azad University, Qaemshahr, Iran

electrical conductivity [5–11]. Conducting polymeric sensors are more important than other sensors because of their high sensibility, fast response and superior mechanical properties at ambient temperature. The capacity of these polymers to interaction with different gases introduces them as promising sensors [2, 4]. The performance of conducting polymers as sensor is important since some molecules in air are rather poisonous and their present can be dangerous for healthiness such as headache and breathing difficulty. Conducting polymeric sensors are very inexpensive compared to semiconductor transistor [12], metal semiconductors in oxide form and some other systems [13].

Among mentioned polymers, polyaniline (PANI) is attractive for the clarification; could be simply manufactured and also could profitably be used at ambient temperature [14, 15]. Furthermore, PANI could be mixed by nanoparticles to form nanocomposite and so it has high surface area to obtain high-quality interaction with some gases. It was found that PANI could be used in the form of nano-fiber gas sensors [16]. There are different reaction mechanisms for PANI in literatures [7, 17–19]. For example Li et al. [18] prepared PANI nanofibers and used it for detection of aromatic organic compounds. Pinto et al. [19] used sulfonic acid-doped PANI nanofiber as sensors towards various aliphatic alcohol vapors and found good responses, particularly for larger chain of alcohol.

It is proven that molecular simulations give significant information on the concept of different adsorbent-adsorbate systems [5–11, 20–25]. As an example, Habib et al. [4] used DFT Study of PANI emeraldine salt towards sensing of some gases. They founded that this sensor has greater selectivity toward NH_3 compared to other gases.

Hydrogen cyanide (HCN) is one of the most dangerous gases at room temperatures and could consequently be breathed in. So, an air breathing apparatus should be used in the present of HCN. There are some ab-initio DFT modeling studies in literatures focusing on HCN adsorption at different states [9, 26, 27]. As an example, Somayeh et al. [27] investigated the sensitivity of siliceous and aluminum doped graphene sheets toward HCN. They reported that aluminum doped graphene is more sensitive to HCN than siliceous doped grapheme. In our previous study [9] the sensitivity of Terpyrrole as a model for polypyrrole toward toxic hydrogen cyanide (HCN) has been studied using DFT but we found low adsorption energy for that.

To the best of our knowledge, sensing behavior of PANI for HCN has not been studied both theoretically and experimentally. We have achieved first-principles calculations to go around the adsorption behavior of the HCN on 2PANI. We used orbital analysis including density of states (DOS) to find any possible hybridization between HCN and 2PANI upon adsorption process. As a result, PANI can be used to design a helpful and very cheap sensor for HCN.

2 Computational methods

All geometric structures were completely optimized using Gaussian 09 program package [28]. We used DFT method including 6-31+G(d,p) basis set by applying BLYP density functional including a version of Grimme's D dispersion model [29]. Moreover to have a comparison, we used M06-2X/6-31+G (d,p) level of theory for another optimization. The UV–vis spectra of pristine 2PANI and 2PANI-HCN complex were simulated at time-dependent-BLYP-D/6-31+G (d,p) level of theory. Two rings of oligomer were selected and permitted to be relaxed to its lowest energy structure based on aforementioned basis set. The ends of molecule capped with hydrogen atoms to counterbalance the valances of corner nitrogen. Additionally we used periodic boundary conditions at BLYP-D/6-31+G (d,p) level of theory to achieving the value of adsorption energy of HCN on PANI at the best configuration resulted by adsorption of HCN on 2PANI. The gap of energy between the HOMO and LUMO for pristine 2PANI is calculated to be 4.59 eV. The released energies of HCN molecule during adsorption on 2PANI at different configurations were calculated based on Equation (1). The corrected counterpoise method [30] for calculation of energy is shown in Equation (2).

$$E_{\text{ads}} = E_{\text{HCN-2PANI}} - (E_{\text{HCN}} + E_{\text{2PANI}}) \tag{1}$$

$$E_{\text{ads, CP}} = E_{\text{ads}} - E_{\text{BSSE}} \tag{2}$$

where E_{ads}, $E_{\text{HCN-2PANI}}$, E_{HCN}, E_{2PANI}, E_{BSSE} and $E_{\text{ads, CP}}$ are the adsorption energy of HCN on 2PANI, the energy of HCN-2PANI complex, the energy of an isolated HCN, the energy of a pristine 2PANI, the energy of basis set superposition errors, and counterpoise adsorption energy, respectively. The amount of charge transfer between HCN molecule and 2PANI is calculated using the variation of the electric charge on HCN upon interaction with 2PANI. This computation is carried out by natural bond orbital charge analysis (NBO).

3 Results and discussion

3.1 Optimized geometry of 2PANI

Geometry optimization of 2PANI has been done at DFT- BLYP-D/6-31+G(d,p) level of theory and is shown in Figure 1. For relaxed structure of isolated 2PANI, the lengths of N. . .H bond is calculated to be 1.01 Å TS[a] with bond angle ($\angle C_{16}N_{21}C_4$) of 127.76° and dihedral angle ($\angle C_{16}N_{21}C_4C_5$) of 144.6°, respectively.

TS[a] Please check and confirm unit.
TS[b] Please check and confirm the short running title.

Editor's or typesetter's annotations (will be removed before the final TEX run)

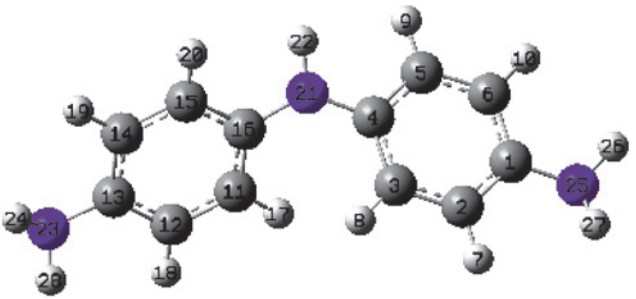

Figure 1: Optimized structure of 2PANI.

3.2 Optimized geometry of 2PANI-HCN and calculation of adsorption energy

To deep understanding the sensitivity of PANI sensor, geometry optimizations of different configurations of 2PANI-HCN system were carried out at the same basis set. As input files we considered different possible orientations of HCN-2PANI interaction: the H or N-sides of HCN closes to the N or H-site of 2PANI. We used full optimization for any initial configurations. After fully optimization we achieved 3 relaxed structures denoted as P1, P2 and P3 (see Figure 2). Optimized geometric parameters and E_{ads} (kcal/mol) are summarized in Table 1.

The intra-molecular H. . .N distance ($d_{N21\cdots H22}$) for each configuration is different compared to that of isolated 2PANI. This is because of the differences in the electro-negativity and dipole moment of different HCN-2PANI complexes.

Our calculated values of adsorption energy show that the HCN molecule could be adsorbed on 2PANI exothermically with adsorption energy of −4.3 kcal/mol (counterpoise corrected energy). This value of HCN adsorption on 2PANI is greater than that of on Terpyrrole (−3.92 kcal/mol, without counterpoised correction) which reported earlier by us [9]. Moreover the value of HCN adsorption in this study is higher than ∼3.6 which is calculated for interaction of methanol with 2PANI reported previously by us [7]. The position P1 is the most appropriate configuration among all three ones because of its larger value of adsorption energy. This relaxed structure explains that HCN interacts through the H side of HCN to the N- site of 2PANI. Also this moderate value of E_{ads} suggests that the interaction between HCN and 2PANI is categorized in the range of physisorption. It may be important to study the impact of different basis functions so we checked it using single point calculations for all before relaxed systems with M06-2X/6-31+G (d,p) level of theory. The results are summarized in supplementary table TS[c]. It is clear from these tables that there are some minor

TS[c] Please check and change. There is no supplementary material available to this article.

Editor's or typesetter's annotations (will be removed before the final TEX run)

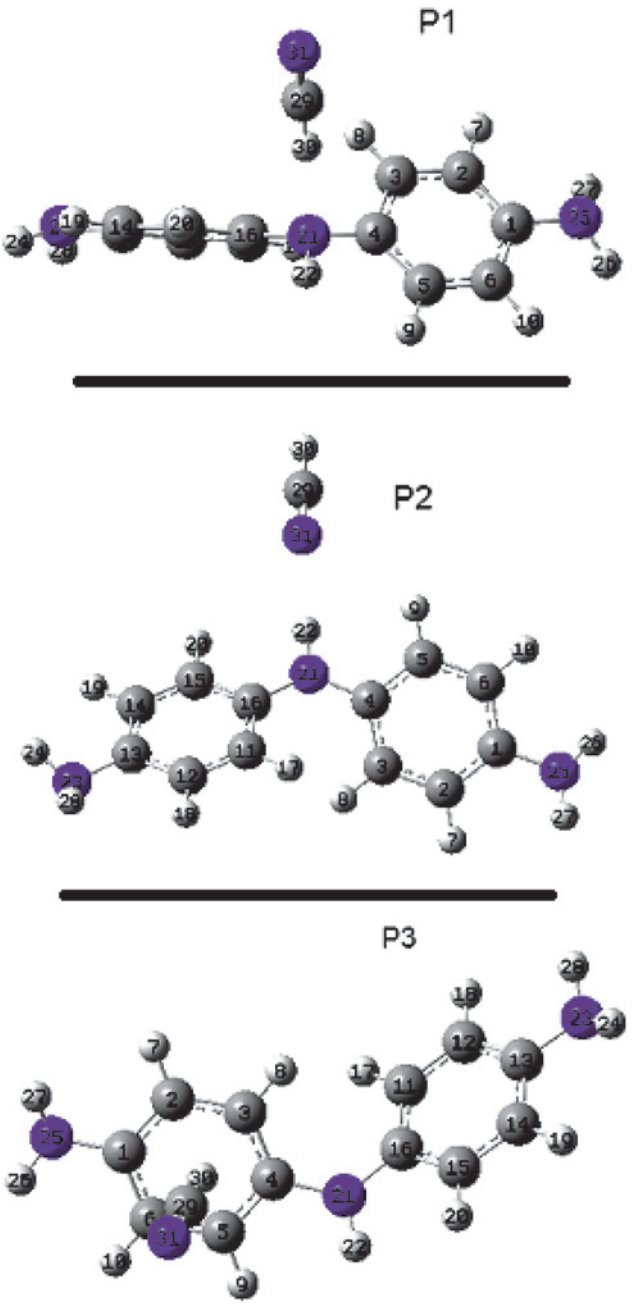

Figure 2: Optimized geometries for three configurations (P1, P2 and P3).

Table 1: Optimized geometric parameters and E_{ads} by means of BLYP-D/6-31+G(d,p). (Bond lengths in Å TS[d] and bond angles in deg)

Configuration	$d_{H22\ldots N31}$	$d_{N21\ldots H22}$	$\angle C_{16}N_{21}C_4$	$\angle C_{16}N_{21}C_4C_5$	$\angle N_{21}H_{22}N_{31}$	E_{ads} kcal/mol	E_{ads} (PBC)[2] kcal/mol
P1	4.62	1.02	121.91	123.46	67.00	−5.4 (−4.3)[1]	2.1
P2	2.25	1.01	128.49	158.62	175.82	−3.5 (2.5)[1]	NA
P3	5.32	1.01	127.67	170.94	88.81	−4.3 (3.2)[1]	NA

[1] Counterpoise corrected energy.
[2] Periodic boundary conditions.

differences between the values of these two methods. The orders of physisorption values of energy as well as the electronic properties are also similar which confirm the original obtained data. We used periodic boundary conditions to achieving the value of adsorption energy upon adsorption of HCN on PANI at the most appropriate configuration (P1) at BLYP-D/6-31+G(d,p) level of theory. As can be seen from Table 1, we calculated the value of −2.11 kcal/mole as the value of absorption energy for interaction of HCN with PANI. Despite the value of adsorption energy for PANI significantly decreased regarding to that of 2PANI, but this value of adsorption still confirms the sensitivity of real PANI to HCN.

TS[d] Please check and confirm unit in Table 1 caption.

Editor's or typesetter's annotations (will be removed before the final TEX run)

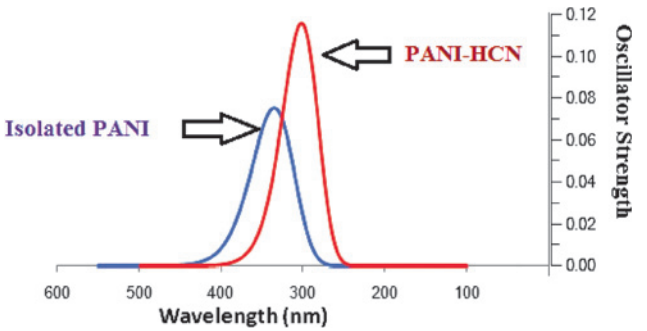

Figure 3: UV-vis spectra of isolated 2PANI and 2PANI-HCN complex.

3.3 UV-vis study

The UV–vis spectra of isolated 2PANI as well as 2PANI-HCN (P1) complex (at the most appropriate orientation) were simulated at time-dependent density functional theory (TDDFT) – BLYP-D/6-31+G (d,p) level of theory and the spectra is given in Figure 3. This is an effective theoretical method towards electronic excitation energies [31].

The experimental band for real PANI is observed at 328–346 nm which is attributed to the chain of the aromatic nuclei and corresponds to the π–π^* transition of the polymeric skeleton [32].

Based on the experimental report, the λ_{max} value of PANI is about 334 nm (3.71 eV) [32], which is 0.10 eV larger than our calculated λ_{max} value (345 nm) for pristine 2PANI (3.61 eV). This acceptable difference is because of infinite numbers of PANI length considered in experimental work while our calculation is simulated based on limit length of polymer with only two rings.

As HCN bounds with 2PANI, the λ_{max} value is red shifted which is due to $\pi \rightarrow \pi^*$ transition. A red shifted of 23 nm in 2PANI is resulted after interaction with HCN which is a consequence of an increase in the band gap. The increase in the band gap of resulted complex of 2PANI-HCN (P1) is confirmed by the results of density of states (DOS) which is discussed at following section. Hence the red shifted value of UV-vis spectra confirms the sensing property of 2PANI for HCN.

3.4 NBO analysis

To search on the alteration in the electronic structures of 2PANI upon interaction with HCN, the net charge transfer (Q) between the 2PANI and HCN was consid-

ered via NBO analysis. Transferring of the electron charge corresponds to a significant function in the electronic properties and also to the performance of interaction. Our calculations showed −0.04, +0.03 and −0.04 e as the net charge transfer between 2PANI and HCN for P1, P2 and P3, respectively (see Table 2). For these calculated charge transfers, the negative value means charge transfer from 2PANI to HCN. In other hand, the positive value means the reverse transfer. The value of charge transfer at the most appropriate configuration of HCN on 2PANI ($-0.04\ e^-$) has quite different than that of reported for Terpyrrole ($+0.03\ e^-$) which studied in our pervious study [9]. It can be conducted that the H atom of HCN molecule is an electron lacking side because of the high electro-negativity of CN group, so it could be anticipated that HCN at P1 and P3 configuration accept charge from the 2PANI. For P2 configuration, 2PANI donates charge to HCN. This finding is in accordance with the larger value of adsorption energy for P1. Also this result reveals that upon interaction of HCN with 2PANI, the electronic properties do not change significantly which point to physical interaction.

3.5 Density of States (DOSs)

To more understand of the electronic properties of HCN/2PANI, the DOSs were calculated near the Fermi level (E_F) for isolated HCN, 2PANI, and 2PANI-HCN complexes at their three positions (see Figure 4). Considering the DOSs of 2PANI to that of 2PANI-HCN, it can be found some confirmations of hybridization between the HCN molecule and 2PANI which confirm the kind of interaction between them. The Fermi level is somewhat changed from −2.14 eV at isolated 2PANI to −2.88, −2.18 and −2.44 eV for HCN-2PANI at configuration P1, P2 and P3, respectively (see Table 2). The key statement for the Fermi level is that in a molecule zero in temperature, it lies in the heart of the HOMO-LUMO gap. It should to be noted that, in fact what lies in the heart of the HOMO-LUMO gap is the chemical potential [22]. The change in the Fermi level causes a change in the work function, which is important in the amount of energy emission. The work function is defined using the standard process by calculating the potential energy variation between the vacuum level and the Fermi level, which actually is the minimum required energy for one electron to be transferred from the Fermi level to the vacuum [31]. It can be found that the alteration in the work function changes the field emission properties of 2PANI.

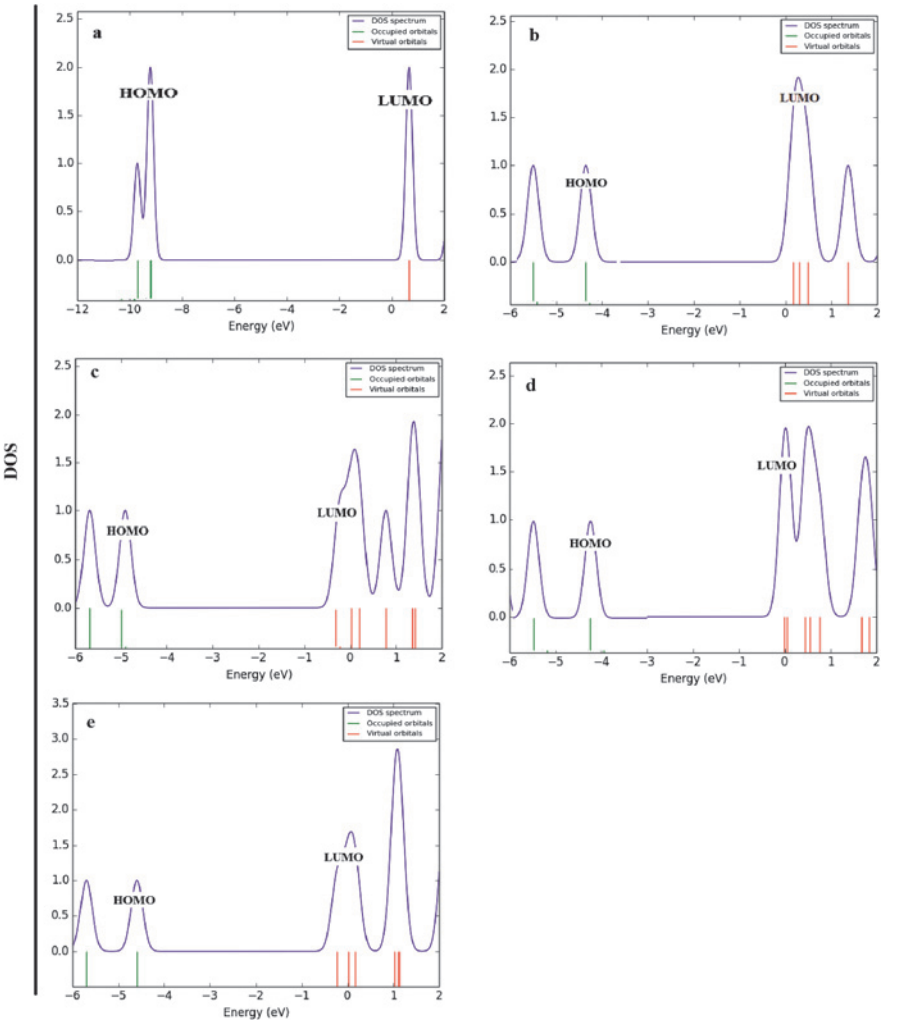

Figure 4: DOSs of different systems: isolated HCN (a), isolated 2PANI (b), 2PANI-HCN (P1) (c), 2PANI-HCN (P2) (d), and 2PANI-HCN (P3) (e).

3.6 Quantum molecular description

The HOMO-LUMO distribution for any complex (2PANI-HCN) may helps better understanding of interaction. The HOMO known an electron donor since it has excess of electrons; whereas the LUMO known as wanting of electrons [12, 13]. The change in the energy of HOMO and LUMO of isolated 2PANI upon adsorption of HCN confirms the kind of interaction. After interaction of HCN with 2PANI, sig-

Table 2: Calculated binding energy (E_{ads}), charge transfer (Q), E_{HOMO}, E_{LUMO}, the energy of Fermi level (E_{FL}) and the HOMO/LUMO energy gap (E_g).

System	Q_{NBO} (e)	E_{HOMO} (eV)	E_{FL} (eV)	E_{LUMO} (eV)	E_g (eV)
HCN	–	−9.77	−4.60	0.56	10.33
2PANI	–	−4.26	−2.04	0.171	4.43
2PANI-HCN (P1)	−0.04	−4.91	−2.57	−0.23	4.68
2PANI-HCN (P2)	0.02	−3.94	−1.97	−0.009	3.93
2PANI-HCN (P3)	−0.03	−4.59	−2.4	−0.22	4.37

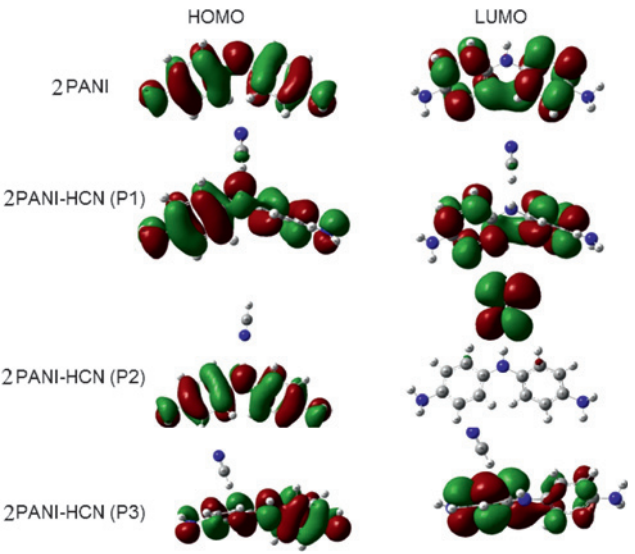

Figure 5: HOMO and LUMO of isolated 2PANI and 2PANI-HCN at three configurations (P1, P2 and P3).

nificant changes occurred in its HOMO and LUMO energies. While 2PANI interacts with acidic nature molecules, we can see an increase in the energy of HOMO.

The quantum molecular descriptions for interaction of HCN with 2PANI are presented in Table 2. Also the distributions of HOMO-LUMO orbitals were presented in Figure 5. Based on the quantum description, the interaction of two reactants is for the reason of interaction of frontier molecular orbitals [23, 24]. The HOMO and LUMO of HCN and 2PANI before and after interaction were given in Table 2.

As they listed in Table 2, the value of E_g ($E_{HOMO} - E_{LUMO}$) of 2PANI increases on mixing with HCN for P1 and decreases for P2 and P3. For P1 configuration,

increasing in the energy band gap is a result of decreasing electron density (HCN admit electron from 2PANI). In other hand, for P2 configuration any decrease in the energy of band gap is attributed to increasing electron density (swap electron to HCN) which is in accordance to our charge analysis results. For P3 configuration, albeit there is negative charge for HCN but little decrease of energy band gap was seen.

4 Conclusion

Our calculation was based on DFT calculations to realization the geometric and electronic structure of 2PANI-HCN at different configurations to observe the mechanism of interaction of 2PANI with HCN. Based on our calculation the interaction of HCN with 2PANI causes to release $-4.3\ \text{kcal mol}^{-1}$ (based on counterpoise corrected energy). Geometries of the isolated 2PANI and HCN are different considerably than those of 2PANI-HCN complexes. After complex formation, the bond angle ($\angle C_{16}N_{21}C_4$) and dihedral angle ($\angle C_{16}N_{21}C_4C_5$) were altered depending on the type of configuration. Electronic properties simulation such as UV-vis analysis, NBO charge analysis, energy band gap, and quantum molecular description confirmed the sensing ability of 2PANI toward HCN. The results of DOSs reveal some minor orbital hybridizing between HCN and the 2PANI cause to physisorption.

Acknowledgement: The authors highly acknowledge financial support from Islamic Azad University, Qaemshahr Branch, Iran.

References

1. J. W. Y. Lam and B. Z. Tang, Acc. Chem. Res. **38** (2005) 745.
2. H. Ullaa, K. Ayub, Z. Ullah, M. Hanif, R. Nawaz, A.Ali Shah, and S. Bilal, Synthetic Met. **172** (2013) 14.
3. B. Wang and M. R. Wasielewski, J. Am. Chem. Soc. **119** (1997) 12.
4. H. Ullah, A. Ali Shah, S. Bilal, and K. Ayub, J. Phys. Chem. C **117** (2013) 23701.
5. A. Shokuhi Rad, J. Mol. Model. **21** (2015) 285.
6. A. Shokuhi Rad, N. Nasimi, M. Jafari, D. Sadeghi Shabestari, and E. Gerami, Sensor. Actuat. B-Chem. **220** (2015) 641.
7. A. Shokuhi Rad and P.Valipour, Synthetic Met. **209** (2015) 502.
8. A. Shokuhi Rad, P. Valipour, A. Gholizade, and S. E. Mousavinezhad, Chem. Phys. Lett. **639** (2015) 29.

9. A. Shokuhi Rad, M. R. Zardoost, and E. Abedini, J. Mol. Model. **21** (2015) 273.
10. A. Shokuhi Rad, Mol. Phys. **114** (2016) 584.
11. S. S. Liu, L. J. Bian, F. Luan, M. T. Sun, and X. X. Liu, Synthetic Met. **162** (2012) 862.
12. K. Natori, J. Appl. Phys. **76** (1994) 4879.
13. J. W. Grate, Chem. Rev. **100** (2000) 2627.
14. L. J. Bian, J. H. Zhang, J. Qi, X. X. Liu, D. Dermot, and K. T. Lau, Sensor. Actuat. B-Chem. **147** (2010) 73.
15. F. W. Zeng, X. X. Liu, D. Diamond, and K. T. Lau, Sensor. Actuat. B-Chem. **143** (2010) 530.
16. S. H. Hosseini and A. A. Entezami, Polym. Advan. Technol. **12** (2001) 482.
17. R. A. Potyrailo, C. Surman, S. Go, Y. Lee, T. Sivavec, and W. G. Morris, J. Appl. Phys. **106** (2009) 6.
18. W. Li, N. D. Hoa, Y. Cho, D. Kim, and J. S. Kim, Sensor. Actuat. B-Chem. **143** (2009) 132.
19. N. J. Pinto, I. Ramos, R. Rojas, P. C. Wang, and A. T. Johnson, Sensor. Actuat. B-Chem. **129** (2008) 621.
20. A. Shokuhi Rad, A. Shadravan, A. A. Soleymani, and N. Motaghedi, Curr. Appl. Phys. **15** (2015) 1271.
21. A. Shokuhi Rad and O. R. Kashani, Appl. Surf. Sci **355** (2015) 233.
22. A. Shokuhi Rad, Synthetic Met. **209** (2015) 419.
23. A. Shokuhi Rad, Appl. Surf. Sci. **357** (2015) 1217.
24. A. Shokuhi Rad, Synthetic Met. **210** (2015) 171.
25. A. Shokuhi Rad, Surf. Sci. **645** (2016) 6.
26. C. Chen, M. H. Liu, and L. S. Wu, J. Mol. Struct.-THEOCHEM **630** (2003) 187.
27. F. R.Somayeh, A. A. Peyghan, and N. L. Hadipour, Appl. Surf. Sci. **265** (2013) 412.
28. Gaussian 09, Revision D.01, M. J. Frisch, G. W. Trucks, H. B. Schlegel, G. E. Scuseria, M. A. Robb, J. R. Cheeseman, G. Scalmani, V. Barone, B. Mennucci, G. A. Petersson, H. Nakatsuji, M. Caricato, X. Li, H. P. Hratchian, A. F. Izmaylov, J. Bloino, G. Zheng, J. L. Sonnenberg, M. Hada, M. Ehara, K. Toyota, R. Fukuda, J. Hasegawa, M. Ishida, T. Nakajima, Y. Honda, O. Kitao, H. Nakai, T. Vreven, J. A. Montgomery, Jr., J. E. Peralta, F. Ogliaro, M. Bearpark, J. J. Heyd, E. Brothers, K. N. Kudin, V. N. Staroverov, R. Kobayashi, J. Normand, K. Raghavachari, A. Rendell, J. C. Burant, S. S. Iyengar, J. Tomasi, M. Cossi, N. Rega, J. M. Millam, M. Klene, J. E. Knox, J. B. Cross, V. Bakken, C. Adamo, J. Jaramillo, R. Gomperts, R. E. Stratmann, O. Yazyev, A. J. Austin, R. Cammi, C. Pomelli, J. W. Ochterski, R. L. Martin, K. Morokuma, V. G. Zakrzewski, G. A. Voth, P. Salvador, J. J. Dannenberg, S. Dapprich, A. D. Daniels, Ö. Farkas, J. B. Foresman, J. V. Ortiz, J. Cioslowski, and D. J. Fox, Gaussian, Inc., Wallingford, CT (2009).
29. S. Grimme, J. Antony, S. Ehrlich, and H. Krieg, J. Chem. Phys. **132** (2010) 154104.
30. S. F. Boys and F. Bernardi, Mol. Phys. **19** (1970) 553.
31. Y. Zhang, Y. Duan, and T. Wang, Phys. Chem. Chem. Phys. **47** (2014) 26261.
32. A.R Vera, B.H Romero, and E. Ahumada, J. Chil. Chem. Soc. **48** (2003) 1.